Boreal carbon loss due to poleward shift in low-carbon ecosystems
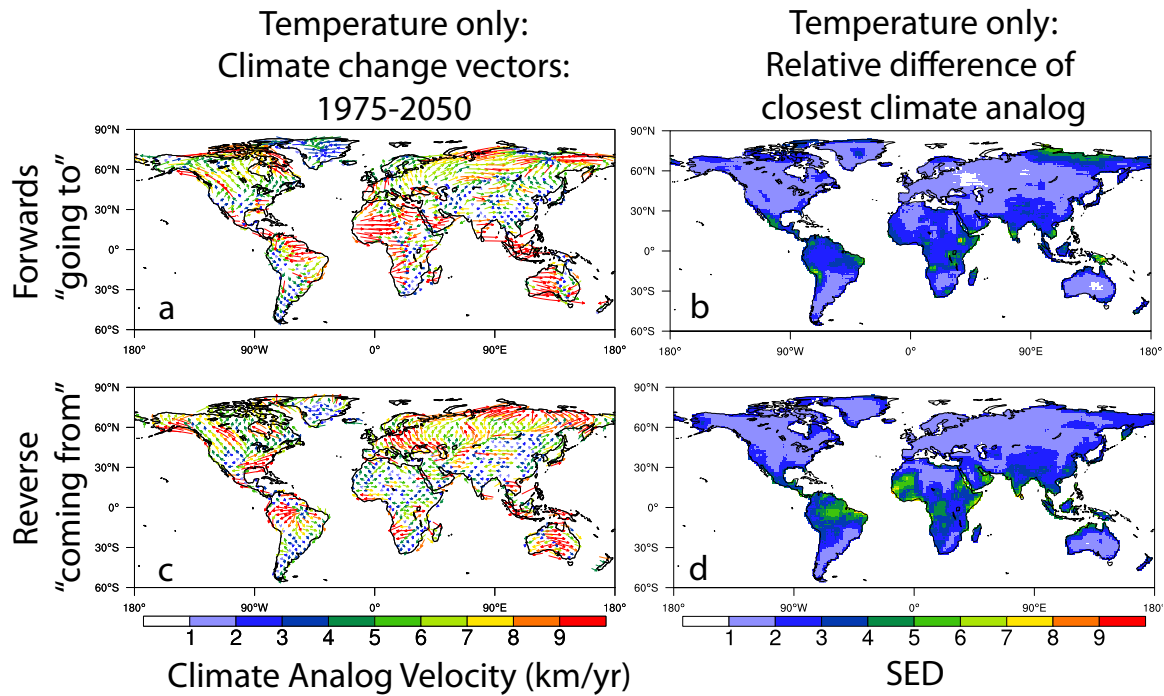### Supplementary Figures

C. D. Koven

Figure S1: Climate analog velocity vectors and agreement, as in figure 1, but calculated using 12 monthly-mean temperature values only.
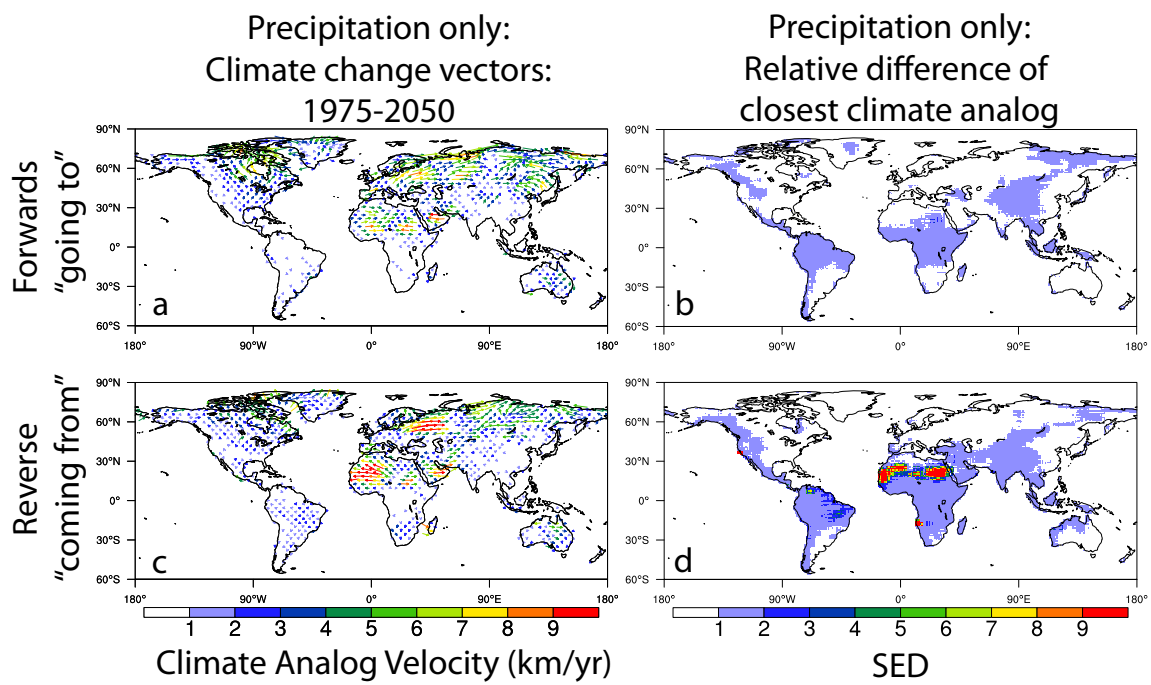
Figure S2: Climate analog velocity vectors and agreement, as in figure 1, but calculated using 12 monthly-mean precipitation values only.
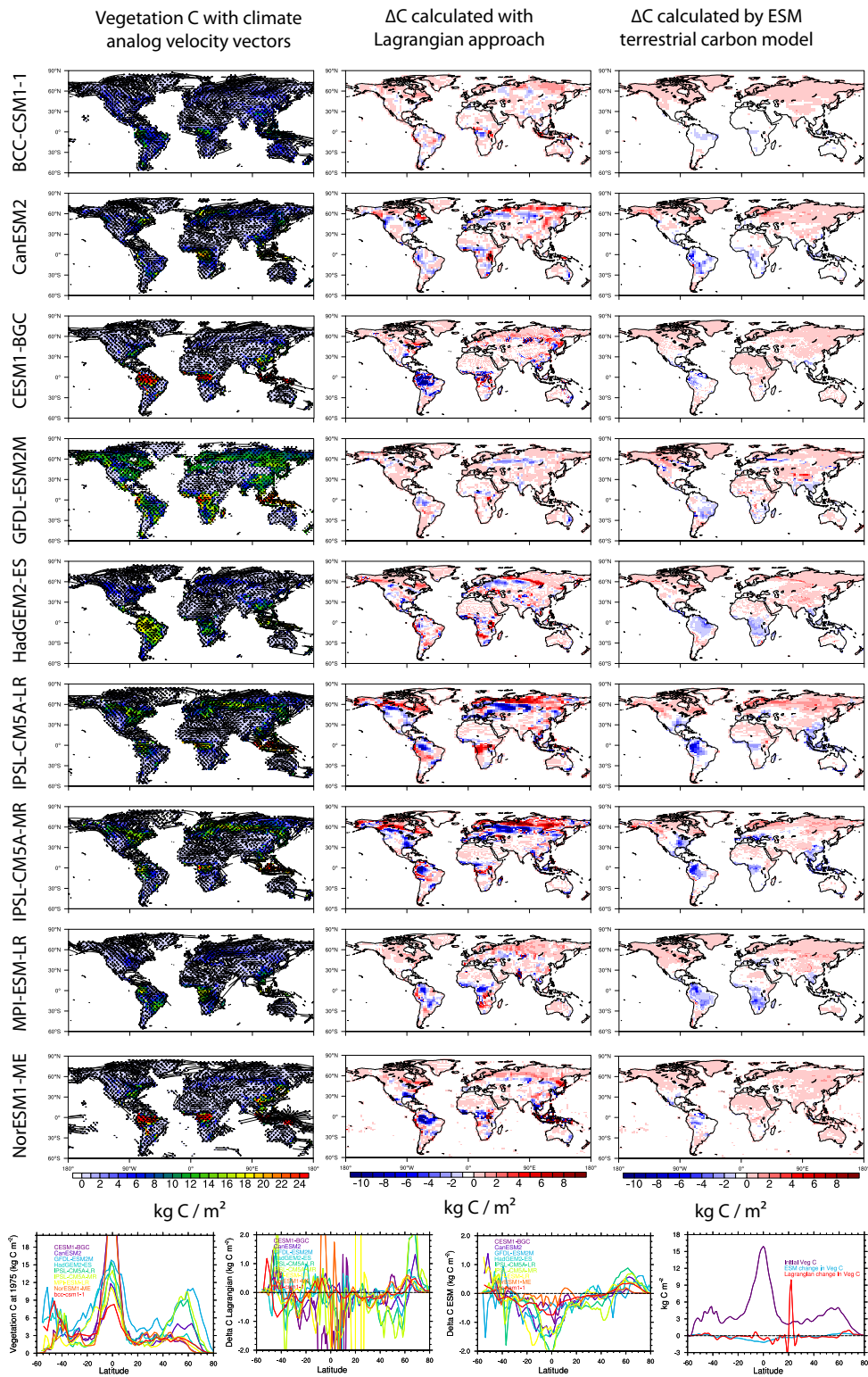
Figure S3: Lagrangian and ESM C changes, as in fig. 2, for all models reporting results for the CMIP5 esmfdbk1 experiment, which uses 1% CO2 increase per year rather than the RCP4.5 scenario used in esmfdbk2. The historical carbon distribution and climate were diagnosed from years 45-74 and the warmed climate years 111-130. The patterns are similar to those shown in figure 2. Key differences due to the fact that land-use was not included in the esmfdbk1 experiment can be seen in Europe and Eastern US, where the carbon gain is smaller here since the regrowth of forests on formerly agricultural land is not included; and in E and SE Asia where current and future anthropogenic forest carbon losses are not included.
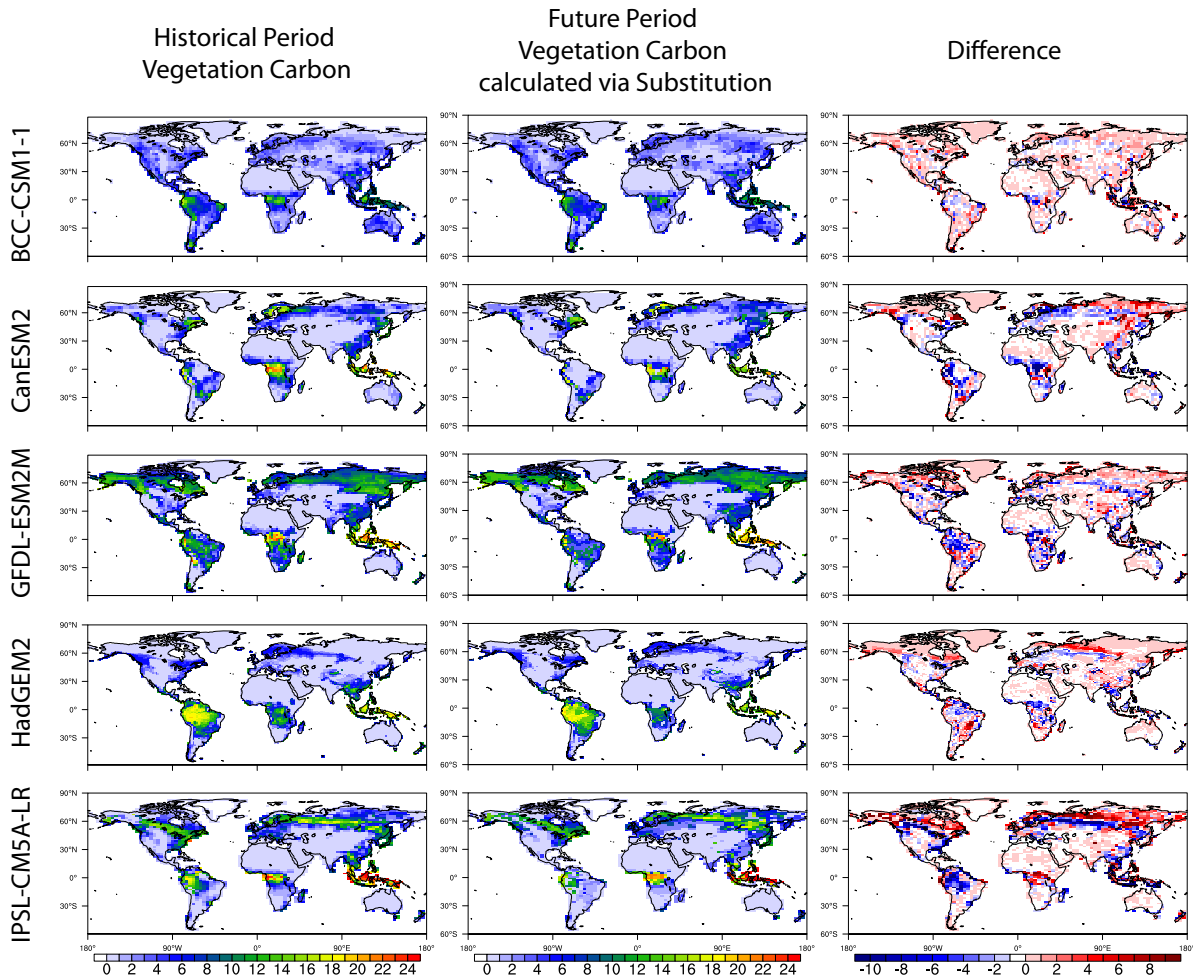
3

Figure S4: Carbon change calculated via direct substitution of C from historical analog gridcell into corresponding future climate gridcell. The magnitude and spatial pattern of carbon change is similar to that in fig. 2; thus the carbon changes calculated based on transport along current spatial gradients are representative of expected equilibrium changes through substituting carbon values from the closest analog climate.